Effect of YAG Laser Cutting on Stretch-flangeability of TRIP-aided Dual-phase Steel Sheets*

Akihiko NAGASAKA,** Atsushi MIO*** and Kazuhide WADA***

The effect of YAG laser cutting on the stretch-flangeability of transformation-induced plasticity (TRIP)-aided dual-phase sheet steels (TDP steels), which had different contents of C, Si and Mn, was examined. In TDP steels in which Si and Mn contents were constant and C content was varied ((0.1−0.4)C−1.5Si−1.5Mn, mass%), the strength − stretch-flangeability balance ($TS \times \lambda$) of holes obtained by either laser cutting, hole-punching or drilling decreased with increasing C content. When the C content was 0.3 mass% or higher, the λ value in the case of laser cutting, which originally was as good as that in the case of drilling, decreased to a level comparable to that in the case of hole-punching. On the other hand, in TDP steels in which Si and Mn contents were varied and C content was kept constant (0.2C−(1.0−2.0)Si−(1.0−2.0)Mn, mass%), the λ value of the hole obtained by hole-punching was low under high *TS*; however, the value was greatly improved by laser cutting. Based on the above results, we demonstrated that YAG laser cutting contributes to the improvement of the stretch-flangeability of 980-MPa-class TDP steels with 0.2 mass% C.

Key words: YAG laser cutting, retained austenite, transformation-induced plasticity, stretch-flangeability.

1. Introduction

Among the high-strength steels developed recently for the purpose of reducing the weight of automotive structural parts and improving shock safety, TRIP-aided dual-phase sheet steels (TDP steels), in which TRIP[1] of retained austenite (γ_R) is effectively utilized, has superior press formability.[2−5] Therefore, the application of the TDP steels for use as suspension parts, such as the lower arm, where the weight reduction effect is high, and impact absorption parts, such as the front-side member, has been examined.[6]

The authors reported that it is possible to improve the relatively low stretch-flangeability, compared to other press formabilities, of TDP steels through warm forming and the use of second-phase morphology.[7−15] In this study, in order to improve the stretch-flangeability of TDP steels, the effect of YAG laser cutting on the stretch-flangeability of TDP steels, the effect of TDP steels was examined.

2. Experimental Procedure

As-cold-rolled steels (steel thickness: 1.2 mm) with different contents of C, Si and Mn were used as specimens (Table 1). After intercritical annealing,[5, 15] the specimens were subjected to austempering to obtain TDP steel composed of ferrite (α_f)+bainite (α_b)+γ_R, as shown in Fig. 1. For comparison of the results, α_f+martensite (α_m) dual-phase sheet steel (MDP steel, 0.14C−0.21Si−1.74Mn, mass%) and $\alpha_f+\alpha_b$ dual-phase sheet steel (BDP steel) were also prepared.[5]

For the tensile test, JIS-13B tensile specimens were used with a crosshead speed of 1 mm/min (strain rate 2.8×10^{-4} /s). Hole-expanding tests were conducted, using disk specimen of 50 mm in diameter and experimental apparatus illustrated in Fig. 2. After holes with 5 mm initial diameter were processed by laser

Table 1. Chemical composition of steels used (mass%).

Steel	C	Si	Mn	P	S	Al
L	0.10	1.49	1.50	0.015	0.0012	0.038
A	0.21	1.51	1.00	0.015	0.0013	0.041
B	0.20	1.51	1.51	0.015	0.0011	0.040
C	0.20	1.49	1.99	0.015	0.0015	0.039
E	0.20	1.00	1.50	0.014	0.0013	0.038
F	0.18	2.00	1.50	0.015	0.0013	0.037
N	0.29	1.46	1.50	0.014	0.0012	0.043
P	0.40	1.49	1.50	0.015	0.0012	0.045

* Retouch correction of ICOMAT '2002; June 10−14, 2002

** Associate Professor, Department of Mechanical Engineering

*** First Technical Section

Received May 17, 2002

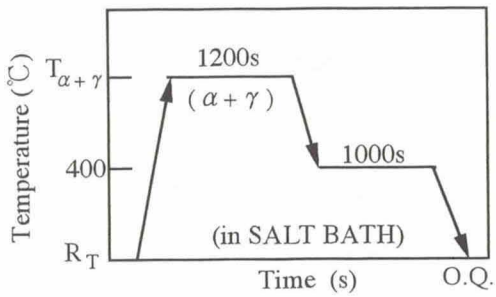

Fig. 1. Heat treatment diagram of TDP steel, in which "O.Q." and "$T_{\alpha+\gamma}$" represent quenching in oil and intercritical annealing temperature, respectively.

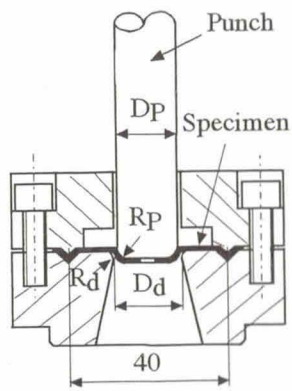

(D_p=17.4 mm, R_p=3 mm, D_d=22 mm, R_d=1 mm)

Fig. 2. Experimental apparatus for expanding.

cutting, hole-punching or drilling, they were finished by flat-bottom punching. For laser cutting, a pulse YAG laser apparatus was used. The conditions of laser cutting were as follows: pulse energy 4 J/P; pulse width 2 ms; pulse frequency 25 Hz; feed speed 100 mm/min. Oxygen gas was used as an assist gas (0.5 MPa). The stretch-flangeability was evaluated using the hole-expanding ratio $\lambda=(d_f-d_0)/d_0\times100\%$. Here, d_0 and d_f represent the initial diameter of the holes and the diameter at which cracks occur, respectively.

The volume fraction of the retained austenite was quantified by X-ray diffractometry using Mo-Kα radiation (five-peak method).[16] In addition, the initial carbon concentration in the retained austenite ($C_{\gamma 0}$, mass%) was estimated from the lattice parameter ($a_{\gamma 0}$, nm) measured from the (220)γ diffraction peak of Cr-Kα radiation using the following equation.[17]

$$C_{\gamma 0}=(a_{\gamma 0}-0.35467)/4.67\times10^{-3} \quad \cdots\cdots (1)$$

3. Results and discussion

3.1 Structure and tensile properties

Figure 3 shows scanning electron micrograph of steel B. Table 2 summarizes the volume fraction of retained austenite ($f_{\gamma 0}$), carbon concentration in retained

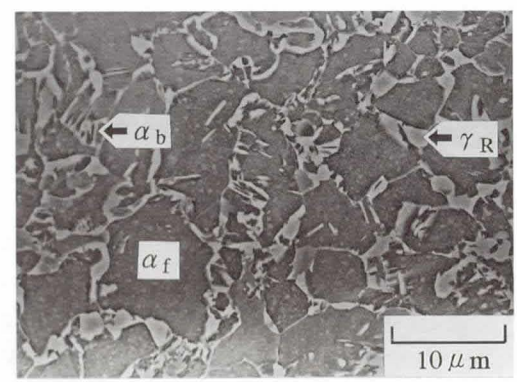

Fig. 3. Scanning electron micrograph of steel B, in which "α_f", "α_b" and "γ_R" are ferrite matrix, bainite island and retained austenite particle, respectively.

Table 2. Retained austenite characteristics and tensile properties.

Steel	$f_{\gamma 0}$	$C_{\gamma 0}$ (mass%)	M_S (℃)	*YS* (MPa)	*TS* (MPa)	*UEl* (%)	*TEl* (%)	*TS*×*TEl* (GPa%)	*RA* (%)	*n*	*r*
L	0.049	1.31	−12	429	651	27.8	37.2	24.2	49.2	0.25	0.89
A	0.058	1.51	−54	470	742	27.2	32.3	24.0	56.6	0.25	0.94
B	0.090	1.38	−37	526	825	31.7	36.0	29.7	44.0	0.22	0.72
C	0.137	1.26	−24	516	984	20.4	22.9	22.5	43.1	0.23	0.84
E	0.076	1.41	−48	494	767	24.6	29.0	22.2	52.4	0.23	0.92
F	0.085	1.31	−12	517	911	27.8	31.9	29.1	44.5	0.30	0.87
N	0.132	1.41	−45	562	895	28.6	32.2	28.8	41.8	0.22	0.97
P	0.170	1.45	−61	728	1103	29.2	32.8	36.2	41.8	0.21	0.90

$f_{\gamma 0}$: volume fraction of retained austenite, $C_{\gamma 0}$: carbon concentration in retained austenite, M_S: estimated martensite-start temperature, *YS*: 0.2% proof stress or yield stress, *TS*: tensile strength, *UEl*: uniform elongation, *TEl*: total elongation, *TS*×*TEl*: strength−ductility balance, *RA*: reduction of area, *n*: work hardening exponent ($\varepsilon=5-15\%$) and *r*: *r*-value ($\varepsilon=10\%$).

austenite ($C_{\gamma 0}$) and tensile properties. From the micrograph, it is clear that a network-like second phase lies mainly on the ferrite grain boundaries in the TDP steels, similarly to the secondary microstructure in the MDP and BDP steels. And the second phase consists of the bainite islands and retained austenite particles, near or apart from the bainite islands. For TDP steel specimens A to F (0.2C − Si − Mn, mass%), $f_{\gamma 0}$ increases with increasing Si and Mn contents, however, $C_{\gamma 0}$ decreases. For TDP steel specimens L to P (C−1.5Si−1.5 Mn, mass%), both $f_{\gamma 0}$ and $C_{\gamma 0}$ increase with increasing C content. TDP steel specimens have high tensile strength (*TS*), large total elongation (*TEl*) and a work hardening exponent (*n*-value) of 0.2 or higher.

3.2 Stretch-flangeability

Figure 4 shows the relationship between tensile strength (*TS*) and hole-expanding ratio (λ). Figure 4(a) shows the relationship for TDP steel with constant Si and Mn contents (1.5 mass%) and 0.1−0.4 mass% C. Figure 4(b) shows that of TDP steel with a constant C content (0.2 mass%) and various Si and Mn contents. As shown in Fig. 4(a), with increasing C content, hole-expanding ratios (λ) of holes obtained by laser cutting, hole-punching or drilling decrease. When C content is 0.3 mass% or higher, the λ value in the case of laser cutting, which originally was as good as that in the case of drilling, decreases to a level comparable to that in the case of hole-punching. Based on the examination of the strength−stretch-flangeability balance ($TS\times\lambda$), which is the product of the tensile strength (*TS*) and hole-expanding ratio (λ), when C content is 0.3 mass% or higher, $TS\times\lambda$ decreases by 50%. As shown in Fig. 4(b), for steel with 0.2 mass% C, the λ value in the case of hole-punching, which tends to decrease under high *TS* such as in the case of steel C, can be improved by laser cutting, as in the case of drilling, enabling a high $TS\times\lambda$ value. The λ values obtained were comparable to that obtained under the combined effect of warm forming and the use of second-phase morphology.[14] Based on the above discussions, we demonstrated that YAG laser cutting contributes to the improvement of the stretch-flangeability of 980-MPa-class TDP steels with 0.2 mass% C.

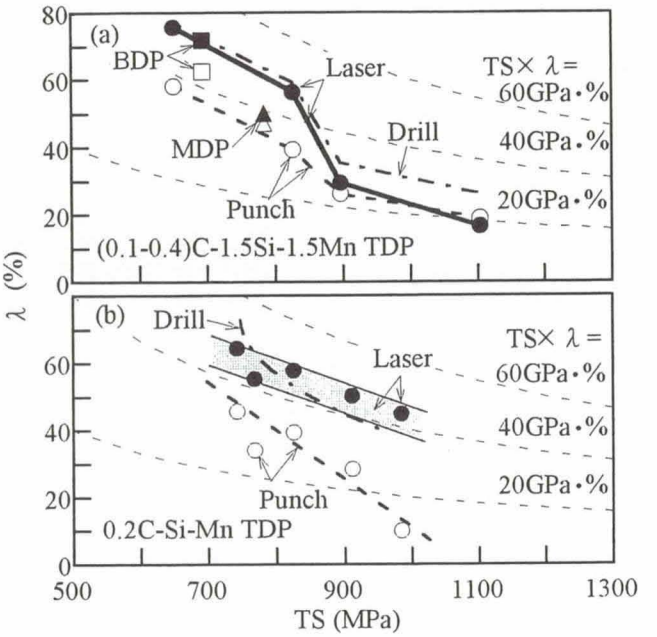

Fig. 4. Comparison of hole-expanding ratio (λ) as a function of tensile strength (*TS*), in which marks represent punching (open marks) and laser cutting (solid marks).

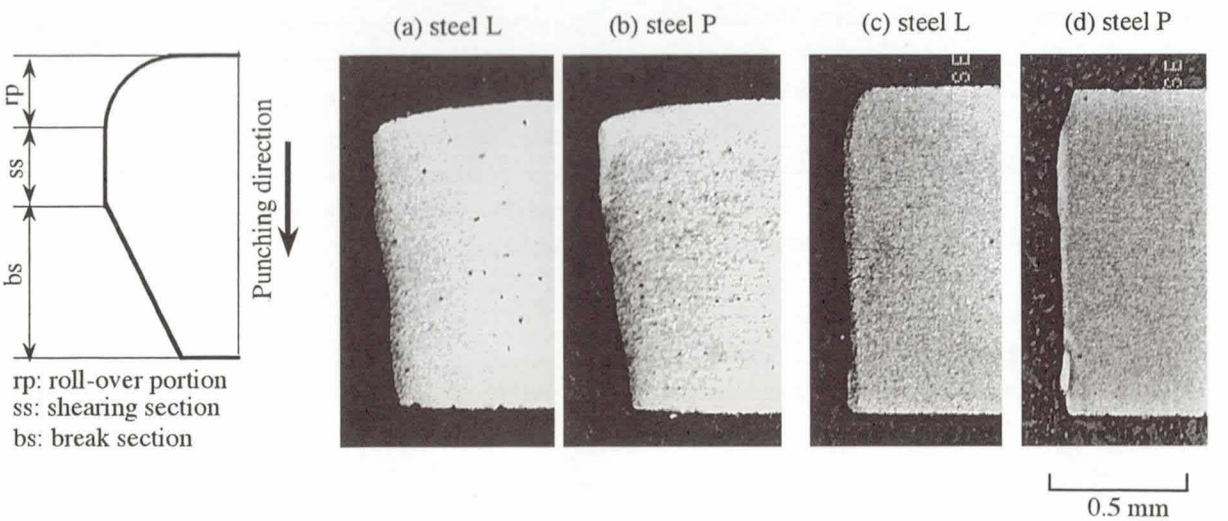

Fig. 5. Optical micrographs of cross-section of TDP steels with (a and b) hole-punching or (c and d) YAG laser cutting.

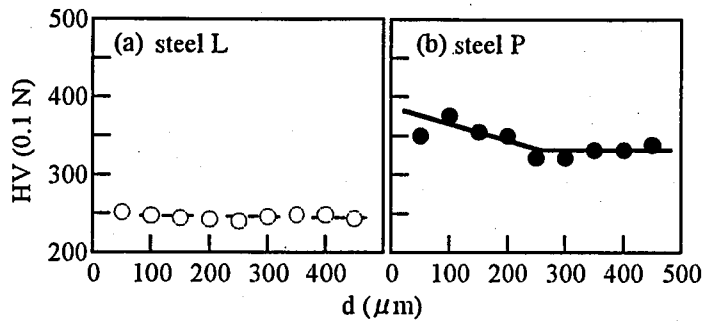

Fig. 6. Variation in Vickers hardness (*HV*) at the cross section of distance of laser cutting (*d*) in TDP steels.

Figure 5 shows optical micrographs of the cross section of TDP steels after hole-punching and laser cutting. Figures 5(a) and 5(b) show the cross sections of steels L and P with different C contents after hole-punching, respectively, and Figs. 5(c) and 5(d) show those of the same specimens after laser cutting. In general, in the case of hole-punching, a roll-over portion (*rp*), shearing section (*ss*) and break section (*bs*) are formed along the direction of punching. With increasing C content, the shearing section length decreases. This leads to an increase in the length of break sections and a decrease of the λ value (Fig. 4(a)). However, in the case of specimens subjected to laser cutting, no distinct differences in *rp*, ss or *bs* were observed.

3.3 Mechanism of stretch-flangeability improvement by laser cutting

Figure 6 shows the Vickers hardness (*HV*) distributions directly below the laser-cut cross section of TDP steels. As shown in Fig. 6(a), the hardening layer formed by laser cutting is nominal in steel L, however an approximately 250-μm-thick hardening layer exists in steel P. This indicates that with increasing C content, the thickness of the hardening layer increases. The hardening layer was composed of a partially melted zone and a heat-affected zone (HAZ), and cracks were observed. Here, the concept of a weld zone is applied. Since the hardness of martensite itself varies with C content, the hardness of the HAZ changes, leading to a greater influence of base metal on the low-temperature crack sensitivity.

Figure 7 shows the relationship between the carbon equivalent (*CEN*) and the strength−stretch-flangeability balance ($TS \times \lambda$). Here, the carbon equivalent was calculated using the following equation.[18]

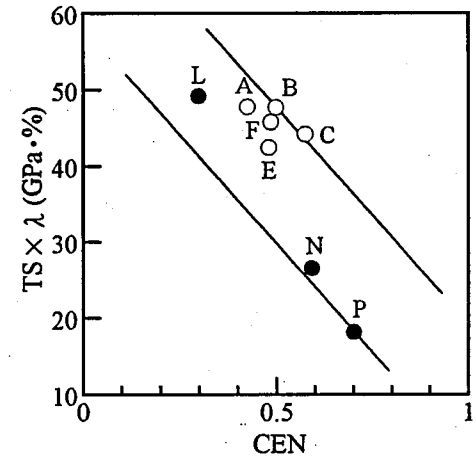

Fig. 7. Correlation between strength−stretch-flangeability balance ($TS \times \lambda$) and carbon equivalent (*CEN*), in which marks represent C−1.5Si−1.5Mn TDP steel (solid marks) and 0.2C−Si−Mn TDP steel (open marks).

The solid and open circles correspond to TDP steels with varied and constant (0.2 mass%) C contents, respectively. As shown in the figure, a negative correlation is observed, which indicates that the carbon equivalent level is one of the factors in the reduction of the stretch-flangeability. When C content is 0.2 mass%, the $TS \times \lambda$ value is 40 GPa·% or higher, which is considered to correspond to the threshold value of the laser cutting effect on stretch-flangeability.

$$CEN = C + A(C)\left\{\frac{Si}{30} + \frac{Mn}{6} + \frac{Cu}{15} + \frac{Ni}{20} + \frac{Cr + Mo + Nb + V}{5} + 5B\right\}$$

$$A(C) = 0.75 + 0.25 \tanh\{20(C - 0.12)\} \quad \cdots\cdots (2)$$

4. Conclusions

The effect of YAG laser cutting on the stretch-flangeability of TDP steels were investigated. The main results were summarized as follows;

(1) In TDP steels with (0.1－0.4)C－1.5Si－1.5Mn (mass%), the strength－stretch-flangeability balance ($TS \times \lambda$) of holes obtained by laser cutting, hole-punching or drilling decreased with increasing C content. When C content is 0.3 mass% or higher, the λ value in the case of laser cutting, which originally was as good as that in the case of drilling, decreased to a level comparable to that in the case of hole-punching.

(2) In the TDP steels with 0.2C－(1.0－2.0)Si－(1.0－2.0)Mn (mass%), the λ value of the hole obtained by hole-punching was low under high *TS*, however, the value was greatly improved by laser cutting. It is considered that the above behavior was due to the fact that the hardening layer directly below the laser-cut surface is extremely thin. The λ value obtained was comparable to that obtained under the combined effect of warm forming and the use of second-phase morphology. The stretch-flangeability of 980-MPa-class TDP steels with 0.2 mass% C was improved by YAG laser cutting.

Acknowledgements

The authors thank Research Foundation for the Electrotechnology of Chubu and The Amada Foundation for Metal Work Technology for their financial support. The authors are grateful to Mr. H. Ito, Mr. S. Imaizumi, Mr. M. Sato, Mr. T. Nakayama and Mr. Y. Harayama, NNCT for useful discussions.

References

[1] V. F. Zackay, E. R. Parker, D. Fahr and R. Busch: Trans. Am. Soc. Met., **60** (1967), 252.

[2] O. Matsumura, T. Ohue and T. Amaike: Tetsu-to-Hagane, **79** (1993), 209.

[3] S. Hiwatashi, M. Takahashi, T. Katayama and M. Usuda: J. Jpn. Soc. Technol. Plast., **35** (1994), 1109.

[4] A. Nagasaka, K. Sugimoto, M. Kobayashi and S. Hashimoto: Tetsu-to-Hagane, **85** (1999), 552.

[5] A. Nagasaka, K. Sugimoto, M. Kobayashi, Y. Kobayashi and S. Hashimoto: Tetsu-to-Hagane, **87** (2001), 607.

[6] Y. Ojima, Y. Shiroi, Y. Taniguchi and K. Kato: SAE Tech. Pap. Ser., #980954, (1998), 39.

[7] O. Matsumura, Y. Sakuma and H. Takechi: Trans. Iron Steel Inst. Jpn., **27** (1987), 570.

[8] K. Sugimoto, M. Kobayashi and S. Hashimoto: Metall. Trans. A, **23A** (1992), 3085.

[9] K. Sugimoto, N. Usui, M. Kobayashi and S. Hashimoto: ISIJ Int., **32** (1992), 1311.

[10] K. Sugimoto, M. Misu, M. Kobayashi and H. Shirasawa: ISIJ Int., **33** (1993), 775.

[11] O. Matsumura, Y. Sakuma, Y. Ishii and J. Zhao: ISIJ Int., **32** (1992), 1110.

[12] K. Sugimoto, M. Kobayashi, A. Nagasaka and S. Hashimoto: ISIJ Int., **35** (1995), 1407.

[13] A. Nagasaka, K. Sugimoto, M. Kobayashi and S. Hashimoto: Tetsu-to-Hagane, **83** (1997), 335.

[14] A. Nagasaka, K. Sugimoto, M. Kobayashi and H. Shirasawa: Tetsu-to-Hagane, **84** (1998), 218.

[15] K. Sugimoto, A. Nagasaka, M. Kobayashi and S. Hashimoto: ISIJ Int., **39** (1999), 56.

[16] H. Maruyama: J. Jpn. Soc. Heat Treat., **17** (1977), 198.

[17] Z. Nishiyama: Martensite Transformation, Maruzen, Tokyo, (1971), 13.

[18] N. Yurioka and T. Kasuya: J. Jpn. Welding Soc., **13** (1995), 343.